The Effect of Dispersal Patterns on Stream Populations*

Frithjof Lutscher†
Elizaveta Pachepsky‡
Mark A. Lewis§

Abstract. Individuals in streams are constantly subject to predominantly unidirectional flow. The question of how these populations can persist in upper stream reaches is known as the "drift paradox." We employ a general mechanistic movement-model framework and derive dispersal kernels for this situation. We derive thin- as well as fat-tailed kernels. We then introduce population dynamics and analyze the resulting integrodifferential equation. In particular, we study how the critical domain size and the invasion speed depend on the velocity of the stream flow. We give exact conditions under which a population can persist in a finite domain in the presence of stream flow, as well as conditions under which a population can spread against the direction of the flow. We find a critical stream velocity above which a population cannot persist in an arbitrarily large domain. At exactly the same stream velocity, the invasion speed against the flow becomes zero; for larger velocities, the population retreats with the flow.

Key words. nonlocal dispersal, critical domain size, spread speed, drift paradox

AMS subject classifications. 92B05, 45C05, 34K05

DOI. 10.1137/050636152

1. Introduction. Traveling wave theory and bifurcation theory provide different approaches to understanding spatial dynamics in ecology [32]. In this paper we use an integrodifferential equation to show that these approaches can be linked when the model contains advection. Related results for reaction-advection-diffusion equations have been obtained in [37, 33]. Here the biological model is for persistence in a stream with growth, diffusion, and downstream advection. As the advection speed increases to a critical traveling wave speed, the upstream invasion stalls.

Many organisms, ranging from river-dwelling flora and fauna to gut-dwelling bacteria, live in environments with predominantly unidirectional flow. As with simple chemostat residents [36], organisms that persist in the presence of such unidirectional

flow must resist being washed out by their moving surroundings. The success of many organisms in maintaining a foothold, even at high flow rates, has given rise to the so-called drift paradox of persistence in unidirectional flow [27, 28].

While possible solutions of the drift paradox have been discussed in the ecological literature [27, 28, 42, 22], until recently the discussion has lacked quantitative scrutiny in the form of models that can be used to predict the effect of environmental variables on maintaining the population. Two recent papers have begun to remedy this lack and have analyzed conditions for species persistence and population spread into upstream environments, both analytically and numerically. The models used there are PDE systems, such as a single compartment model with growth, advection, and diffusion [37], or a two-compartment model with separate mobile and stationary states corresponding to aquatic and benthic populations [33].

Flows in river systems are very complex and include, for example, up- and down-river currents as well as turbulent long-distance movement of biota [1]. Although systems of PDEs are the workhorse for spatial ecology models in continuous space [15], their application is limited as they depict the complex asymmetrical spatial flow in a river through simple advection and diffusion.

Integrodifferential equations [16] are related to PDEs but encompass more general movement patterns than diffusion and advection. In particular, the modeling formalism can allow for a detailed description of the complicated dispersal that arises through river flow. The added realism of integrodifferential models comes at a price: much of the theory for PDEs on problems such as critical domain size for species persistence [35] or population spread [18] has not yet been formulated for their integrodifferential cousins, but see [26] for invasion speeds. We develop some of the theory needed for analysis in this paper.

In this paper we revisit the drift paradox, employing integrodifferential models that allow us to include long-distance dispersal. We show how the long-distance dispersal changes previous washout predictions [33, 37]: populations can always persist under high flow rates, providing rare, long-distance dispersal events are sufficient to allow maintenance of a foothold in the river. Our results contrast with those of Lockwood, Hastings, and Botsford [24], where long-distance dispersal is discounted as playing a role in determining population persistence. While our model and application are new, we draw on theoretical ideas that have a distinguished history in the theory of spatial ecology.

The critical domain size is a fundamental ecological quantity that gives the minimal size of a habitable area required for species survival. In turn, it provides an important tool in reserve design and conservation [6, 8]. The first models for the critical domain size using diffusion equations date back to the 1950s [35, 17]. The analysis has since been extended to cover more complex spatial domains [9], the influence of advection [29, 33], and discrete-time integrodifference equations [20, 41, 25].

Another relevant ecological metric is the speed of spread, which is important in a wide range of ecological applications. While some invasions are intended, such as the introduction of biological control agents [4], others can be devastating for native species being out-competed by invaders and for species diversity. The spread of diseases is a worldwide problem and can be treated in the same modeling framework [26].

While the idea of having stationary and mobile compartments has recently been used by numerous authors, for example, to model protein movement in a cell nucleus [10], population dynamics with diffusive movement [23, 13], or wavelike movement [14], the idea of coupling such models to asymmetric spatial flow dynamics via advection and diffusion, as in [33], is a recent one (but see [5]).

We start our investigation by presenting a general framework to derive dispersal kernels from mechanistic movement models, and we apply this framework to derive a thin-tailed and a fat-tailed kernel. In section 3 we present the general integrodifferential model and develop the theoretical results on critical domain size and invasion speeds. The following three sections contain the application of the general theory to persistence and spread in streams. Three cases for dispersal kernels are considered: thin-tailed (section 4), a weighted sum of thin-tailed kernels, accounting for short- and long-distance dispersal (section 5), and, finally, fat-tailed (section 6).

2. Modeling Dispersal. In this section, we use a mechanistic approach for individual movement to derive theoretical forms of dispersal kernels. A *dispersal kernel* describes the probability that an individual moves from one location to another in a certain time interval. Such dispersal kernels, also referred to as redistribution kernels or seed shadows, have been measured for many organisms [30]. The mechanistic approach taken here allows for explicit description of the movement process and behavior. We assume that population dynamics happen on a much slower time scale than individual movement and hence can be neglected while deriving the kernel. This separation of time scales occurs frequently, and it is certainly true for stream insects, where dispersal can occur over daily time scales, while significant growth typically requires monthly or yearly time scales. The general theory presented here follows, but significantly extends, the results in [30] and is applied to derive a thin-tailed and a fat-tailed dispersal kernel as specific examples for analysis and further development later in the paper.

We denote $\omega(t, x; y)$ as the probability density of the location of a mobile individual with initial location $x = y$. We assume that the individual moves for a random length of time, T, after which it settles, and that the random variable T has a given probability density $p(t)$. The dispersal kernel is now defined as the probability density of stopping points from given initial location, i.e.,

$$(2.1) \qquad \kappa(x, y) = \int_0^\infty p(t)\omega(t, x; y)dt.$$

If $\omega(t, x; y)$ depends only on the signed distance from the starting point $\xi = x - y$ rather than the exact location, we simply write $w(t, \xi) = \omega(t, x; y)$ and $k(\xi) = \kappa(x, y)$. Most dispersal kernels in this paper are of this form. For an exception, see Appendix E. When the individual moves by Brownian motion with diffusion coefficient D, the function $w(t, x)$ is the fundamental solution of the heat equation on the real line,

$$(2.2) \qquad w(t, x) = \frac{\exp\left(\frac{-x^2}{4Dt}\right)}{\sqrt{4\pi Dt}}.$$

When drift at rate v is included with the Brownian motion, the function $w(x, t)$ is given by (2.2) with x replaced by $x - vt$.

However, if dispersing individuals can jump long distances in short time intervals, the Brownian motion model may not be valid. For example, the Lévy flight model [11] assumes that arbitrarily large jumps can occur over short time scales. The result is a distribution of jump distances which has no variance. In this "anomalous diffusion" case, a typical form for w is the Cauchy distribution

$$(2.3) \qquad w(t, x) = \frac{t}{\rho\pi}\left[\left(\frac{x}{\rho}\right)^2 + t^2\right]^{-1}.$$
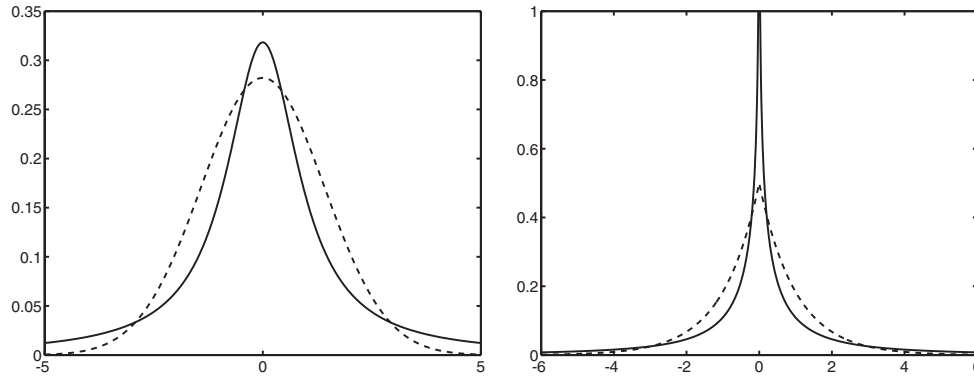
Fig. 2.1 *The plot on the left shows the thin-tailed Gaussian (dashed) and fat-tailed Cauchy (solid) distribution as given in (2.2) and (2.3) for $t_0 = 1$ with parameters $D = 1$ and $\rho = 1$, respectively. The plot on the right shows the Laplace distribution (2.6) (dashed) and the fat-tailed distribution (2.7) (solid). Parameters are as above and the settling rate is $\alpha = 1$. Note that the fat-tailed distribution has a singularity at the origin.*

The parameter ρ has dimension [space/time] and stands for an effective speed. Details of how (2.3) can be derived from a random walk model for individuals are given in Appendix A. As above, we introduce drift at rate v by replacing x with $x - vt$.

We now turn to modeling the stopping time T. The simplest possible assumption is that all individuals disperse for the same, fixed, length of time t_0. In this case

$$(2.4) \qquad p(t) = \delta(t - t_0),$$

so that (2.1) yields $k(x) = w(x, t_0)$. Thus, for a fixed dispersal time t_0, the dispersal kernel (2.1) is simply the Gaussian (2.2), possibly shifted if $v \neq 0$, or the Cauchy distribution (2.3), again possibly shifted if $v \neq 0$, evaluated at time t_0. In Figure 2.1, we plot the shapes of these kernels.

A more general form of stopping times comes from defining $\alpha(t)$ as the *settling* or *failure rate* [38], i.e., $\alpha(t)\,dt$ as the probability that the individual ends its movement during $[t, t + dt]$. The probability density for the stopping times of the individual, also called the lifetime probability density, is then

$$(2.5) \qquad p(t) = \alpha(t) \exp\left(- \int_0^t \alpha(s)\,ds\right).$$

The argument of the exponential function is known as the *hazard function* [38].

For constant settling rate α, the dispersal kernel (2.1) is the Laplace transform of the probability density ω with respect to time. In the case of Brownian motion (2.2), the kernel (2.1) becomes the Laplace distribution [7],

$$(2.6) \qquad k(\xi) = \sqrt{\frac{\alpha}{4D}} \exp\left(-\sqrt{\frac{\alpha}{D}}|\xi|\right).$$

For constant settling rate α and the Cauchy redistribution function (2.3), the kernel (2.1) becomes the fat-tailed kernel

$$\begin{aligned} (2.7) \qquad k(\xi) &= \theta\,\Re\left\{E_1(i\theta\xi)\exp(i\theta\xi)\right\}/\pi \\ &= -\theta\left(\cos(\theta\xi)\,\mathrm{ci}(\theta\xi) + \sin(\theta\xi)\,\mathrm{si}(\theta\xi)\right)/\pi, \end{aligned}$$

where $\theta = \alpha/\rho$. The functions E_1, ci, and si are the exponential, cosine, and sine integrals, respectively,

(2.8)
$$\mathrm{E}_1(x) = \int_1^\infty \frac{\exp(xz)}{z}\,dz, \quad \mathrm{ci}(x) = -\int_1^\infty \frac{\cos(xz)}{z}\,dz, \quad \mathrm{si}(x) = -\int_1^\infty \frac{\sin(xz)}{z}\,dz.$$

The kernels given by (2.6) and (2.7) are plotted in Figure 2.1.

Adding drift into the last two scenarios does *not* simply shift the kernels (2.6) and (2.7) as it did above but instead causes a different kind of asymmetry in dispersal, as we show later. In section 4.1, we employ a somewhat simpler method to derive the kernel for Brownian motion with drift. The case of Lévy flight with drift is done in section 6.

In Appendix B we generalize the simple model of Brownian motion to the case of two (and potentially more) dispersal modes. Individuals switch between these modes. We show that corresponding dispersal kernels can be derived explicitly for constant settling rate.

3. The Model Equation, Critical Domain Size, and Spread Speed. In this section, we present the general model for a population subject to population dynamics and spatial movement. It has the form of an integrodifferential equation, for which we give alternative derivations. We then state the main assumptions and prove formulas for the critical domain size and the spread speed of the population.

We consider a single population, which is described by its density $u(t,x)$. Population dynamics such as birth and death of individuals are summarized in the function $f(u)$. Then the dispersal time scale is small compared to the population dynamics time scale; dispersal can be modeled by a position-jump process with jumping rate μ [31]. If an individual jumps, the dispersal kernel $\kappa(x,y)$, as discussed in section 2, describes the probability that the individual moves from some point y to x. Then the evolution of the population density is governed by the following integrodifferential equation:

(3.1)
$$u_t(t,x) = f(u(t,x)) - \mu u(t,x) + \mu \int_\Omega \kappa(x,y)u(t,y)dy.$$

The domain of integration Ω will depend on the question we study. In the case of the critical domain size, it will be a bounded interval; in the case of invasion speeds, it will be the real line. Although the model formulation is valid in spatial domains of any dimension, we will restrict ourselves to the one-dimensional case since the applications below will be to systems with unidirectional flow. We assume that the function f is a single-hump function, i.e., $f(0) = f(\bar{u}) = 0$, and $f > 0$ on $(0, \bar{u})$. To prove Theorem 3.2, we will need more assumptions on f and k, which we state then.

There are several ways to derive (3.1). We present a novel approach emphasizing the separation of time scales. Then we present the necessary theoretical results about the critical domain size and invasion speeds.

3.1. Model Derivations. Besides the derivation in [31], (3.1) is derived in the ecological literature from a random walk process with variable move length [40]. Reaction and movement are assumed to be on the same time scale [12]. Recently, a very careful derivation of (3.1) has been presented where some scaling issues have been avoided [16].

Here, we present an alternative derivation that respects and even relies on the fact that movement often happens on a much faster time scale than population dynamics. We start by dividing the population into stationary and mobile classes, u

and v, respectively, and assume that birth and death processes affect only stationary individuals. Stationary individuals start moving with rate μ, and mobile individuals settle with rate σ. Then we obtain the system

$$(3.2) \qquad u_t = f(u) - \mu u + \sigma v, \qquad v_t = G[v] + \mu u - \sigma v,$$

where G is a differential operator describing movement, e.g., $G = D\Delta$ (diffusion) or $G = D\Delta - V\nabla$ (advection and diffusion). Recently, there has been increasing interest in this or similar systems [5, 10, 13, 23, 33]. To apply the quasi steady-state assumption that movement happens on a much faster time scale than population dynamics, we introduce the scaling parameter $\varepsilon = \mu/\sigma$ and rescale v and G in (3.2) to obtain

$$(3.3) \qquad u_t = f(u) - \mu u + \mu \tilde{v}, \qquad \varepsilon \tilde{v}_t = \tilde{G}[\tilde{v}] + \mu u - \mu \tilde{v},$$

where ˜ denotes the rescaled quantities. Under the quasi steady-state assumption $\varepsilon \to 0$, the equation for $\tilde{v}$ gives the linear differential operator

$$(3.4) \qquad \mu u = \left(\mu - \tilde{G} \right) \tilde{v}.$$

System (3.2) becomes (3.1), with $\kappa(x, y)$ denoting the Green's function of (3.4), i.e.,

$$(3.5) \qquad \tilde{v}(x) = \int \kappa(x, y) u(y) dy.$$

3.2. Critical Domain Size. As a first step in the analysis of (3.1), we now study the critical domain size problem. We find that parameter space can be divided into two parts: one that allows persistence independently of domain size and dispersal kernel, and one in which persistence depends on these two factors. We assume that there is no immigration into the domain. A population will persist if it grows at low density; therefore, we study conditions such that the zero steady state is unstable. The linearization of (3.1) on the interval $[0, L]$ is given by

$$(3.6) \qquad u_t(t, x) = (r - 1)u(t, x) + \int_0^L \kappa(x, y) u(t, y) dy,$$

where we have rescaled time by the rate of movement μ and abbreviated $r = f'(0)/\mu$ as the rescaled growth rate at low density. From (3.6), we immediately see that if $r > 1$, then the zero steady state is unstable *independent* of the domain size and the kind of movement individuals perform. On the other hand, if $r < 1$, then the stability of the zero solution depends on the integral expression in (3.6). We assume that the integral operator

$$(3.7) \qquad I[\phi](x) = \int_0^L \kappa(x, y) \phi(y) dy$$

has a unique simple dominant eigenvalue ν for an appropriate choice of function space. In Appendix C, we discuss possible choices and show the following result.

THEOREM 3.1. *Assume that κ is independent of L. The unique simple dominant eigenvalue ν of (3.7) is a strictly increasing function of the domain length L. Next, assume $f(0) = 0$ and $f'(0) > 0$. Then the zero steady-state solution of (3.1) is unstable, provided $\nu(L) > 1 - r$.*

The condition that κ be independent of L means that dispersing individuals do not perceive domain boundaries or at least do not alter their movement behavior there—for example, aquatic individuals in a river stretch without breaks (source, mouth, waterfall) or in a no-fishing zone, or wind-dispersed seeds. In those cases, the dispersal kernel derived on the infinite domain is simply cut off at the domain boundaries [41]. If the movement behavior is altered at the boundary, then the kernel will depend on L (see Appendix E). Then the first statement of the theorem is shown by showing that the smallest eigenvalue of the differential operator (3.4) is a decreasing function of L. In general, this follows from standard arguments; however, in the special case of zero-flux boundary conditions at both ends (i.e., no loss from the domain) this eigenvalue is independent of L.

According to the theorem, the critical domain size is given by $\nu(L) = 1 - r$. In the original nonscaled parameters, the population can persist if

$$(3.8) \qquad f'(0) > \mu(1 - \nu).$$

Condition (3.8) is a refinement of the unconditional persistence in the case $r > 1$, which we found above. Its interpretation gives a possible explanation of the drift paradox as follows. If the population growth rate at low density, $f'(0)$, exceeds the rate at which individuals move, μ, then the population will always persist, independent of the length of the domain and the kind of movement. In particular, the population can persist in an environment with unidirectional flow. This conclusion was also reached as one possible explanation of the drift paradox in [33]. If $f'(0)$ is smaller than μ, then persistence depends on the term $(1 - \nu)$. As the leading eigenvalue, ν asymptotically gives the fraction of individuals that remains in the domain during dispersal, and consequently, $(1 - \nu)$ is the fraction of individuals leaving the domain due to dispersal. Therefore, if the rate at which individuals move times the probability that they leave the domain during dispersal exceeds the population growth rate, then the population will go extinct. A similar switch from conditional to unconditional persistence in a PDE system was found in [13] (without advection) and [33] (with advection).

3.3. Spread Speed. In the previous section, we analyzed population persistence on a bounded domain. Here, we look at population spread into an unbounded, previously uninhabited domain. We first derive the *minimal speed of a traveling wave* of the linearized system (3.6). We follow the usual line of argument, emphasizing the direction in which the wave is moving [26]. In systems with unidirectional flow, the spread in the direction of the drift will be faster than against the drift. This asymmetry requires some modification in the definition of the *asymptotic spreading speed* [3] for the nonlinear model. After we give the modified definition, we show in Theorem 3.2 that the minimal traveling wave speed and the asymptotic spreading speed coincide.

To determine the wave speed of the linear system, we assume that the kernel is of the form $\kappa(x, y) = k(x - y)$ and change to traveling wave coordinates, $z = x - ct$, where c is the speed of a traveling wave. Then (3.6) gives the following equation for the profile ψ of a traveling wave:

$$(3.9) \qquad -c\psi'(z) = (r - 1)\psi(z) + \int k(z - w)\psi(w)dw.$$

In this linear equation, we make the exponential ansatz $\psi(z) = e^{-sz}$, with $s > 0$ ($s < 0$), such that asymptotically, $\psi \to 0$ as $z \to \infty$ ($z \to -\infty$). After canceling equal

terms on both sides, we get the characteristic equation

$$(3.10) \qquad sc + 1 - r = \int_{-\infty}^{\infty} k(w)e^{sw}dw =: M(s)$$

for $s \neq 0$, where M stands for the moment generating function of k. We will always assume that advection points to the right. Therefore, waves with positive c travel in the direction of advection, and waves with negative c travel against the advection. From (3.10), which will be of use later, the minimal wave speeds are derived as in [26] and given by

$$(3.11) \qquad c^+ = \inf_{s>0} \frac{r - 1 + M(s)}{s}, \quad c^- = \sup_{s<0} \frac{r - 1 + M(s)}{s}$$

for waves with decreasing (c^+) and increasing (c^-) profile. Here, we assume that the moment generating function exists at least for some interval containing zero. In section 6, we discuss the case of a kernel whose moment generating function does not exist except at $s = 0$.

The representation (2.1) of the dispersal kernel for arbitrary settling rate (see (2.5)) is particularly useful in connection with formula (3.11) because the moment generating function of the Gaussian distribution is known. Since the moments of k involve integration in the spatial variable only and since the stopping times are independent of the spatial location, the moment generating function of k is given by

$$(3.12) \qquad M(s) = \int_0^{\infty} p(t) \exp(Dts^2)dt.$$

The concept of the asymptotic spreading speed (henceforth simply referred to as spread speed) for the nonlinear equation was introduced by Aronson and Weinberger [3] and has since been explored in many publications; see [39]. To accommodate for asymmetric spread, we define spread speeds $c_\pm^*$ by the condition

$$(3.13) \qquad \lim_{t\to\infty} u(t, x + ct) = \begin{cases} \bar{u}, & c_-^* < c < c_+^*, \\ 0, & c < c_-^* \text{ or } c > c_+^*, \end{cases}$$

where $\bar{u} > 0$ is the positive zero of f, i.e., $f(\bar{u}) = 0$.

THEOREM 3.2. *Assume that f satisfies $f(0) = 0 = f(\bar{u})$ for some $\bar{u} > 0$, $f'(0) > 0$, and the subtangential condition $f(u) \leq f'(0)u$. Assume that the kernel satisfies the technical conditions stated in Appendix* D. *Then the spread speeds of the nonlinear equation* (3.1) *are given by* (3.11), *i.e., $c_\pm^* = c^\pm$.*

The proof of this theorem in Appendix D uses the upper bound for the spread speed from [26]. To show that the upper bound equals the lower bound, we construct subsolutions of (3.11) adapting the proof in [2] for a simple epidemic model.

4. A Model with Unidirectional Flow. We now apply the general model (3.1) to study systems with unidirectional flow and the influence of the flow on the critical domain size and the spread speed. The biological system motivating our study is a population of aquatic insects in streams, and our results give possible explanations of the drift paradox. At first, we derive an appropriate dispersal kernel. Then we compute the critical domain size as well as the spread speeds with and against the flow direction. We show that these two important ecological characteristics are related as follows. The spread speed against the flow decreases as the advection increases until,

at some critical advection speed, there is no spread against the flow direction. On the other hand, the critical domain size increases with the advection speed until, at some critical advection speed, it becomes infinite; i.e., the population cannot persist in a domain of any size. We show that the two critical advection speeds, indeed, coincide.

4.1. A Dispersal Kernel with Advection. We derive a dispersal kernel that represents the movement of aquatic insects in streams. The larvae of these insects reside on the bottom of the stream, from where they periodically jump into the water column, where they are subject to the flow. Our submodel for individual movement consists of diffusion and advective flow, and we assume a constant settling rate. We think of advection as representing the drift velocity experienced by the larvae and of diffusion as a first approximation to the variability in flow speed and direction. Denoting $z(t, x)$ as the density of moving individuals, we obtain the equation

$$(4.1) \qquad z_t = D z_{xx} - v z_x - \alpha z,$$

where D is the diffusion constant, v is the advection velocity, and α is the settling rate. Integrating (4.1) over $0 \le t \le \infty$ and applying the initial condition $z(0, x) = \delta(x)$ as well as (B.2), we observe that the dispersal kernel k satisfies

$$(4.2) \qquad \frac{D}{\alpha} k_{xx} - \frac{v}{\alpha} k_x - k = -\delta,$$

i.e., k is the Green's function from (3.2). The characteristic equation of (4.2) is $Da^2 - va - \alpha = 0$ with solutions $a_1 > 0$ and $a_2 < 0$, given by

$$(4.3) \qquad a_{1,2} = \frac{v}{2D} \pm \sqrt{\frac{v^2}{4D^2} + \frac{\alpha}{D}}.$$

Using the asymptotic boundary conditions for $x \to \pm\infty$ and the matching condition at $x = 0$, we find that k is of the form

$$(4.4) \qquad k(x) = A \exp(a_1 x), \quad x \le 0, \quad \text{and} \quad k(x) = A \exp(a_2 x), \quad x \ge 0.$$

The value of the constant A is determined by the condition $\int_{-\infty}^{\infty} k(x) dx = 1$, which leads to

$$(4.5) \qquad A = \frac{a_1 a_2}{a_2 - a_1} = \frac{\alpha}{\sqrt{v^2 + 4\alpha D}}.$$

Alternatively, this kernel can be expressed by substituting $x \to x - vt$ in (2.2), $\alpha = $ const. in (2.5), and inserting the result in (2.1). In the special case $v = 0$, the Laplace kernel (2.6) results. We plot the shape of k in Figure 4.1 for different values of v while keeping D, α constant. In Appendix E, we contrast the kernel derived here for an infinite domain with a kernel on a finite domain with mixed boundary conditions of the same type as in [33, 37].

4.2. Critical Domain Size. From the previous section we know that the population persists unconditionally if $r > 1$. For $r < 1$, we have to find L such that $\nu(L) = 1 - r$; see (3.8). This can be calculated analytically. In Appendix F, we convert the integral equation (C.1) into a differential equation, extending earlier work for symmetric kernels [20, 41], and obtain the following expression for L in terms of the eigenvalue ν and the dispersal related constants $a_{1,2}$ from (4.3):

$$(4.6) \qquad L = \frac{4 \arctan \left(\sqrt{\frac{4a_1 |a_2|}{\nu(a_1 - a_2)^2} - 1} \right)^{-1}}{(a_1 - a_2) \sqrt{\frac{4a_1 |a_2|}{\nu(a_1 - a_2)^2} - 1}}.$$
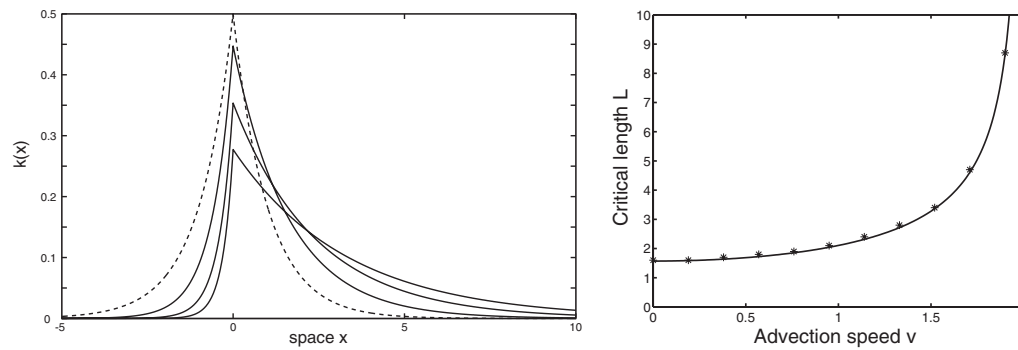
Fig. 4.1 *The picture on the left shows the dispersal kernel* (4.4) *with* $D = 1$, $\alpha = 1$, *and* $v = 1, 2, 3$ *in decreasing height of the peak, solid lines. For comparison, the symmetric kernel for* $v = 0$ *is plotted as the dashed line. The plot on the right gives the critical domain size as a function of the advection as in* (4.6). *The parameters are* $D = 1$, $\alpha = 1$, *and* $r = 0.5$. *The solid line is the analytical expression* (4.6), *and asterisks are numerical results computing the eigenvalue of the integral operator* (C.1), *using Simpson's rule on* 1401 *data points in the interval* $[0, 1]$.

Setting $\nu = 1 - r$, we can hence determine the critical domain size, which we plot in Figure 4.1 as a function of the advection speed v. As expected, the critical domain size is an increasing function of advection speed. From the plot, it appears that $v = 2$ is the critical advection speed, above which the population cannot persist in a domain of any length. In (4.6), L approaches infinity as the square root in the denominator approaches zero. Hence, the critical advection speed is defined by

$$(4.7) \qquad \nu = 1 - r = \frac{4\frac{\alpha}{D}}{\frac{v^2}{D^2} + 4\frac{\alpha}{D}}.$$

For the set of parameters above, $v = 2$ is indeed the critical advection speed.

4.3. Spread Speed. We use formulas (3.10) and (3.11) and Theorem 3.2 to determine the speed of spread. The moment generating function for the generalized Laplace kernel (4.4) is given by

$$(4.8) \qquad M(s) = \frac{a_1 a_2}{(a_1 + s)(a_2 + s)}, \qquad -a_1 < s < -a_2.$$

In Figure 4.2, we plot the hyperbola $M(s)$ with y-intercept $M(0) = 1$ for three different values of the advection speed v. According to (3.10), we also plot straight lines with slope c, the propagation speed, and y-intercept $1 - r < 1$. As given in (3.11), we plot these straight lines for minimal values of $|c|$, such that the straight line and the hyperbola have a point in common; i.e., we plot the case that the line is tangent to the hyperbola. The resulting slopes give the minimal wave speed.

We find exactly two tangent lines. One of them (dash-dot line) always has positive slope, independent of the advection speed $v \geq 0$. This slope is the spread speed c^+ in the direction of advection. It increases with advection. For the other tangent line, we distinguish two cases. First note that the hyperbola is always positive since we assume k to be nonnegative. If now $r > 1$, then the y-intercept of the straight line is negative, and hence the (dashed) tangent line will always have negative slope. This slope corresponds to c^-, the spread speed against the advection. That means if $r > 1$,
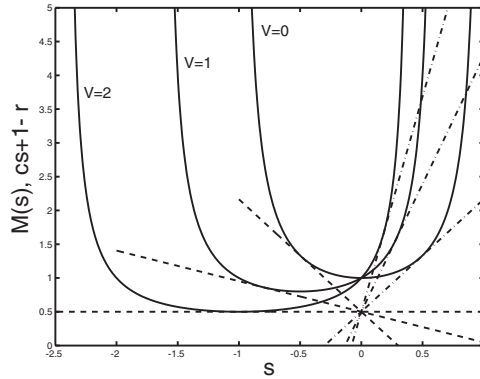
Fig. 4.2 *The hyperbolas are the moment generating function $M(s)$ (4.8) for three different values of v with $D = 1$ and $\alpha = 1$. The straight lines correspond to the left-hand side of (3.10). The slopes of these lines correspond to the spread speeds $c^{\pm}$ according to (3.11). For a more thorough explanation, see corresponding text. For $v = 0$ upstream and downstream spread speed are the same. For $v = 1$ the speed is faster downstream than upstream. For $v = 2$ the upstream spread stops.*

then the population can always invade against the advection. If, on the other hand, $r < 1$, then the tangent line has zero slope if the minimum of $M(s)$ equals $1-r$. If the minimum is smaller than $1 - r$, then also the dashed tangent line has positive slope. Since the slope corresponds to c^-, and since the minimum of $M(s)$ is decreasing with increasing advection, we find a switch in the population's ability to invade against the advection. For small values of $v > 0$, the population can invade against the advection; for large values of $v > 0$, the population retreats with the advection.

To compute the critical advection velocity at which the switch happens, we compute the minimum of $M(s)$ as

$$(4.9) \qquad M\left(-\frac{a_1 + a_2}{2}\right) = -\frac{4a_1 a_2}{(a_1 - a_2)^2} > 0.$$

Therefore, the critical advection speed is given by

$$(4.10) \qquad 1 - r = -\frac{4a_1 a_2}{(a_1 - a_2)^2} \qquad \text{or} \qquad v^2 = 4\frac{r}{1 - r}\,\alpha D.$$

After some rearranging, we find that (4.10) is exactly the same as (4.7). Hence, the advection velocity above which a population cannot persist in a domain of arbitrary length is exactly the same as the advection velocity at which the population stops spreading upstream and starts retreating downstream. This connection between the two ecologically important quantities critical domain size and invasion speed in systems with advection was first hinted at in [37] and then demonstrated in the context of the PDE system (3.2) in [33].

4.4. Upstream Settling Probability. The probabilities that, after a dispersal event, an individual settles down- or upstream from its initial location are given by

$$(4.11) \qquad P_{\text{down}} = \int_0^\infty k(x)dx = \frac{a_1}{a_1 + |a_2|}, \qquad P_{\text{up}} = 1 - P_{\text{down}}.$$

For $r < 1$, we compute a critical upstream-settling probability, below which the population cannot persist or spread against the advection. We insert the critical advection velocity (4.10) into (4.3) and find

$$(4.12) \qquad P_{\mathrm{down}}^* = \frac{1 + \sqrt{r}}{2}, \qquad P_{\mathrm{up}}^* = \frac{1 - \sqrt{r}}{2}$$

as the critical downstream and upstream probabilities, respectively. This result is surprising since the two quantities depend only on the population dynamics parameter and *not* on the movement related parameters α and D. Here lies a chance to test the predictions of the model *without* having to estimate α and D, provided we can estimate P_{up}. Later in the paper (Figure 6.2), we plot the critical domain size as a function of the downstream settling probability and compare it to the case of a fat-tailed kernel.

5. Two Modes of Dispersal. In the case *without advection*, it is known that the shape of the tail of the dispersal kernel has virtually no influence on the critical domain size [24]. On the other hand, the invasion speed for systems without advection crucially depends on the shape of the tail of the dispersal kernel [19]. Even a tiny fraction of long-distance dispersers can have a huge effect on the invasion speed. In the dispersal model of diffusion and settling, longer dispersal distances result from higher diffusion rate or lower settling rate. In the previous section, we showed that in systems *with advection*, there is a close relationship between critical patch size, critical advection velocity, and invasion speed. In this section, we explore how this relationship depends on the shape of the tail of the kernel.

We assume that individuals have two different dispersal modes and choose between those with probabilities p and $1 - p$, respectively. We assume that both dispersal modes can be described by the simple advection-diffusion-settling model (4.1), but with possibly different parameters. Hence, the movement model is given by

$$(5.1) \qquad \begin{aligned} z_{1,t} &= D_1 z_{1,xx} - v_1 z_{1,x} - \alpha_1 z_1, \\ z_{2,t} &= D_2 z_{2,xx} - v_2 z_{2,x} - \alpha_2 z_2 \end{aligned}$$

with initial conditions $z_1(0, x) = (1 - p)\delta(x)$, $z_2(0, x) = p\delta(x)$. Since there is no interaction between the two different dispersal modes, the resulting kernel is simply the weighted sum of the kernels associated with each mode, i.e.,

$$(5.2) \qquad k = (1 - p)k_1 + pk_2,$$

where $k_{1,2}$ are given in (4.4) with the appropriate parameters. We are thinking of the z_2-compartment as the long-distance dispersers; i.e., we want k_2 to have fatter tails than k_1, and we assume that p is small. All other parameters being equal, k_2 will have fatter tails than k_1 if either $D_2 > D_1$ or $\alpha_2 < \alpha_1$. The effect of varying $v_{1,2}$ depends on whether we are looking at the upstream or the downstream direction. For simplicity and to compare the results of this section with those of the previous section, we restrict ourselves to the case $v_1 = v_2$.

We first explore the case of varying D_2 at equal settling rates $\alpha_1 = \alpha_2$. In Figure 5.1 we plot the critical domain size as a function of the advection speed for three different values of D_2 and for fixed $p = 0.1$ We also plot the critical advection speed at which the upstream spread is zero as a vertical line. We observe the following. At low advection speeds, the critical domain size is indeed insensitive to changes in D_2; i.e., it does not depend strongly on the tail of the dispersal kernel. The critical
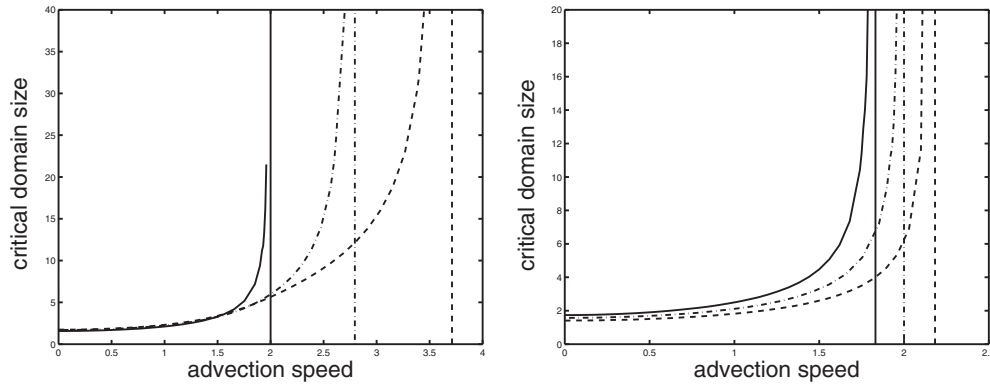
Fig. 5.1 *Left: The critical domain size as a function of the advection speed with dispersal kernel (5.2). The parameters are $D_1 = 1$, $\alpha_1 = \alpha_2 = 1$, $r = 0.5$, $p = 0.1$. The varying parameter is $D_2 = 1$ (solid), $D_2 = 5$ (dash-dot), and $D_2 = 10$ (dashed). The vertical lines give the critical advection speed for upstream invasion from formula (3.10). The values are $v = 2$, $v = 2.7948$, $v = 3.7114$ for $D_2 = 1$, $D_2 = 5$, $D_2 = 10$, respectively. Right: The critical domain size as a function of the advection speed with dispersal kernel (5.2). The parameters are $D_1 = D_2 = 1$, $\alpha_1 = 1$, $r = 0.5$, $p = 0.1$. The varying parameter is $\alpha_2 = 0.1$ (solid), $\alpha_2 = 1$ (dash-dot), and $\alpha_2 = 10$ (dashed). The vertical lines give the critical advection speed for upstream invasion from formula (3.10). The values are $v = 1.8321$, $v = 2$, $v = 2.1833$ for $\alpha_2 = 0.1$, $\alpha_2 = 1$, $\alpha_2 = 10$, respectively.*

domain size increases with increasing D_2, reflecting higher loss at higher diffusion rates. At higher advection speeds, the picture is different. The critical domain size does depend crucially on D_2 and it decreases with increasing D_2. Whereas increasing D_2 increases the loss from the domain downstream, it also increases the probability that a few individuals move upstream. Summarizing in biological terms, at small advection speeds it is important to keep many individuals in the domain; at large advection speeds it is more important to have a few individuals dispersing against the advection. The critical advection speed increases with increasing D_2, which was to be expected since the tails of k get fatter. The curves for the critical domain size approach the straight lines for the critical advection speed for upstream spread, and hence the critical advection speed for persistence and invasion agree, as in the previous section.

Next, we vary the settling rate α_2 at equal diffusion coefficients $D_1 = D_2$. The results are plotted in Figure 5.1, which includes the critical domain size and the critical advection speed for upstream spread just as in the previous plot. The two most important observations are that the curves for different α_2 do not intersect and that the curve with the higher α_2 is always the lower one. Hence, independent of the strength of advection, a higher settling rate always promotes species persistence and the ability to spread upstream. In view of our earlier considerations, this is a surprising result, since decreasing α_2 gives fatter tails of k, yet it reduces the critical advection velocity instead of increasing it, as above when we varied D_2.

There are several ways to explain why increasing D_2 and decreasing α_2, which both produce fatter tails of k_2, have opposite effects on the domain length and the invasion speed. Whereas settling rate and diffusion coefficient appear as a quotient in formulas (2.6), (4.3), which determine the tail of the kernel, they appear as a product in formula (4.10) for the critical velocity of upstream propagation. Increasing D_2

in (4.3) decreases both a_1 and $|a_2|$ to zero, whereas decreasing α decreases $|a_2|$ to zero and a_1 to v/D. Therefore, increasing D_2 makes the kernel more symmetric, whereas decreasing α_2 makes it less symmetric. This can also be seen by computing the skewness of k from (4.4) as

$$(5.3) \qquad -2\frac{v(v^2 + \alpha D)}{(v^2 + 2\alpha D)\sqrt{v^2 + 2\alpha D}},$$

which is a decreasing function in the product αD. In more biological terms, in systems with advection, the probability of moving downstream is higher than the probability of moving upstream. Increasing the diffusion rate increases the probability of moving upstream; increasing the settling rate decreases it. Last, dimensional analysis gives the same result. Characteristic length scales are $\sqrt{D/\alpha}$ for a system without advection and v/α for a system without diffusion. The balance between up- and downstream movement is hence given as

$$(5.4) \qquad \sqrt{D/\alpha} \sim v/\alpha \qquad \text{or} \qquad \alpha D \sim v^2.$$

6. Dispersal by Extremes. In this last section, we explore the ideas from the previous paragraphs in the context of a dispersal kernel whose tails are not exponentially bounded. Such kernels are also known as fat-tailed kernels and describe a situation where long-distance dispersal events are not rare. Different phenomena, such as accelerating invasions, have been shown to occur in that case [19]. We follow the ideas from section 2 to incorporate unidirectional flow in such kernels. Then we numerically investigate how the critical domain size depends on the strength of the flow.

As described in section 2, we compute the appropriate fat-tailed kernel by integrating the Cauchy distribution (2.3) with x replaced by $x - vt$, multiplied with the probability of stopping times (2.5) according to (2.1). This integration yields the asymmetric fat-tailed dispersal kernel

$$(6.1) \qquad k(x) = \frac{\alpha}{(\mu^2 + v^2)\pi}\Re\left((\mu + vi)E_1\left(-\frac{\alpha(v - \mu i)x}{\mu^2 + v^2}\right)\exp\left(-\frac{\alpha(v - \mu i)x}{\mu^2 + v^2}\right)\right).$$

In Figure 6.1 we plot this kernel for various values of v. The critical domain length for the fat-tailed kernel (6.1) is plotted as a function of advection speed in Figure 6.2. As expected, it increases with advection speed but it seems to remain finite even for large v. To compare the results for the fat-tailed kernel here with the results from the asymmetric exponential kernel from section 4, we plot the critical domain length in both cases as a function of the probability of settling upstream from the point of release; see section 4.4. If the advection speed is zero, then the probability of settling upstream from the point of release is 0.5. As the advection speed increases, the probability of settling upstream decreases. In the limit as the advection speed approaches infinity, the upstream probability goes to zero. From the plot in Figure 6.2 we make two observations. The fat-tailed kernel (6.1) produces finite critical domain lengths for smaller upstream probabilities than the exponential kernel; i.e., the population can persist for larger advection speeds. Second, the critical upstream probability for the exponential kernel as computed in (4.12) is independent of the dispersal parameters D and α and depends only on the population growth rate r.
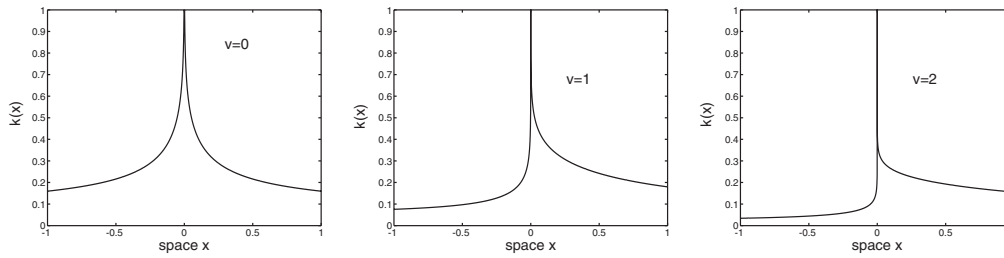
Fig. 6.1 *The fat-tailed kernel from* (6.1) *with parameters* $\mu = 1$, $\alpha = 0.5$ *for different values of advection velocity* v.
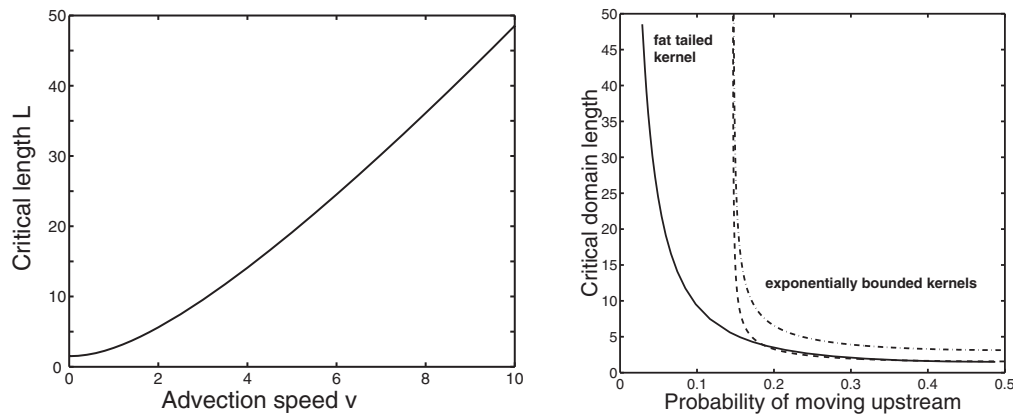

Fig. 6.2 *On the left, the critical domain length for the fat-tailed kernel* (6.1) *is plotted as a function of the advection velocity. The parameters are* $\rho = 1$, $r = 1$, $\alpha = 1$. *On the right, the critical domain length is given as a function of the upstream settling probability. The solid line represents the fat-tailed kernel* (6.1) *with parameters* $\rho = 1$, $r = 1$, $\alpha = 1$. *The dashed and dash-dot lines are for the exponential kernel* (4.4) *with parameters* $\alpha = 1$, $r = 0.5$. *The dashed line corresponds to* $D = 1$, *the dash-dot line to* $D = 4$.

7. Discussion. In this work, we consider integrodifferential models that incorporate population dynamics and individual movement described by dispersal kernels. Extending previous work [30, 33], we consider not only kernels arising from simple random walks but also including (1) unidirectional flow, producing asymmetric kernels, and (2) long-distance jumps (Lévy flight motion), producing fat-tailed kernels. These derivations contribute to the effort to incorporate mechanistic descriptions of individual movement into population models in order to understand the impact of details of individual movement on population dynamics under different conditions.

We obtain general criteria for persistence of a population by deriving the critical domain size for integrodifferential equations. We also extend existing work on the rate of spread [26] and prove that the linear conjecture holds for these systems. Further, we show that in systems with advection there exists a critical advection speed that links population persistence and spread as follows. At a critical advection speed, the population can no longer persist on any finite domain (i.e., the critical domain size is infinite). This critical advection speed is the same as the one that causes upstream propagation to stall (i.e., the upstream propagation speed is 0). We show this result

analytically for the modified Laplace kernel and numerically for other kernels; for related results in a PDE model, see [33].

It has been shown that in systems without advection the shape of tails of the dispersal kernel have little effect on persistence [24] but may be a major determinant of the spread rate of a population [19]. Our results show that in systems with advection, the shape of the tails of kernels influences both. With fat-tailed kernels, a population is able to both persist and spread upstream in conditions with higher flow speed.

Whereas the current model gave us valuable insight into dispersal in stream populations and possible explanations for the drift paradox, we plan to continue these investigations using more realistic biological models. The techniques in this paper will be extended to cover, e.g., resource dynamics and predator-prey interaction. Most important, we plan to model a population of larvae and adult stage where adults emerge from the stream and fly upstream to deposit eggs. This mechanism is the most commonly quoted biological hypothesis to solve the drift paradox. Finally, as we are dealing with low population numbers, we intend to compare the results of these deterministic models to stochastic simulations.

Appendix A. Derivation of the Cauchy Distribution for Individuals Undergoing a Random Walk. The derivation we use follows [11]. Let Y be a random variable, assuming its values on the integer lattice and describing the number of space steps that an individual jumps each time step. The probability that the individual jumps k steps to the right $(\Pr(Y = k) = p_k)$ is defined to be

$$(A.1) \qquad p_k = \begin{cases} 1 - \frac{2m}{\pi} & \text{if} \quad k = 0, \\ \frac{m}{\pi |k|(|k|+1)} & \text{if} \quad k > 0. \end{cases}$$

The parameter m, restricted to $0 < m < \pi/2$, describes the likelihood of dispersing. It is straightforward to show that the p_k sum to one. We produce a random walk on the grid of spacing h with $h > 0$ by letting the walker start at point 0 at instant 0 and defining the location of the individual after n time steps to be

$$(A.2) \qquad X_n = hY_1 + hY_2 + \cdots + hY_n,$$

where Y_n are independent, identically distributed random variables, all having the same distribution as Y. We relate space steps h and time steps τ by the speed s, so $h = s\tau$. At time $t = n\tau = nh/s$ we have $h = ts/n$, so that the spreading time associated with distance X_n is

$$(A.3) \qquad \frac{X_n}{\rho} = \frac{t}{mn}(Y_1 + Y_2 + \cdots + Y_n),$$

where $\rho = ms$ is a speed of spreading. The distribution of the right-hand side of (A.3) converges to the distribution of the normalized Cauchy distribution

$$(A.4) \qquad \frac{1}{\pi}\frac{t}{x^2 + t^2}$$

in the limit as n approaches infinity [11]. Thus X_n approaches (2.3) in the same limit. For any given fixed time t and speed s, the limit n approaching infinity is equivalent to the space step h approaching zero.

Appendix B. Dispersal Kernels for Multiple Dispersal Modes. In extending the simple diffusion model for individual movement, we assume that individuals have two

different modes of dispersal and that they can switch between these modes. We show how the dispersal kernel can be computed explicitly for constant rates and that the kernel is exponentially bounded. The description for individual movement is given by

(B.1)
$$z_{1,t} = D_1 z_{1,xx} - v_1 z_{1,x} - \mu z_1 + \sigma z_2 - \alpha_1 z_1,$$
$$z_{2,t} = D_2 z_{2,xx} - v_2 z_{2,x} - \mu z_2 + \sigma z_1 - \alpha_2 z_2.$$

The parameters D_j, v_j, and α_j are the diffusion rates, the advection speeds, and the settling rates for the different stages. The parameters μ and σ are switching rates between the stages. Initially, there is a certain fraction of the population in each stage, i.e., $z_1(0, x) = p\delta(x)$, and $z_2(0, x) = (1-p)\delta(x)$. The density of stopping points from the respective stages is given by

(B.2)
$$k_j(x) = \int_0^\infty \alpha_j z_j(t, x) \, dt$$

for $j = 1, 2$, and hence the kernel is given by $k(x) = k_1(x) + k_2(x)$.

The case $\alpha_1 = \sigma = 0$ can be interpreted as two successive modes of dispersal. In the case without advection, this has been treated by [30]. If we consider only movement, not settling ($\alpha_{1,2} = 0$), then we can study the shape of the spatial distribution of z_1 and z_2 as it evolves in time. For systems like (B.1) but without advection, Skalski and Gilliam [34] have constructed an explicit solution and computed asymptotic speeds of spread for a linear model.

From (B.1) we deduce that k_1, k_2 satisfy the system

(B.3)
$$-p\alpha_1\delta = D_1 k_1^{(2)} - v_1 k_1^{(1)} - (\mu + \alpha_1)k_1 + \sigma\frac{\alpha_1}{\alpha_2}k_2,$$
$$-(1-p)\alpha_2\delta = D_2 k_2^{(2)} - v_2 k_2^{(1)} - (\sigma + \alpha_2)k_2 + \mu\frac{\alpha_2}{\alpha_1}k_1,$$

where $k_j^{(l)}$ denotes the lth derivative of k_j. Restriction to the interval $(0, \infty)$ and repeated differentiation and substitution of (B.3) yield a fourth-order equation for k_1 as follows:

(B.4)
$$D_1 k_1^{(4)} - \left(v_1 + v_2\frac{D_1}{D_2}\right)k_1^{(3)} - \left(\mu + \alpha_1 - \frac{v_1 v_2 D_1(\sigma + \alpha_2)}{D_2}\right)k_1^{(2)}$$
$$+ \frac{v_1(\sigma + \alpha_2) + v_2(\sigma + \alpha_1)}{D_2}k_1^{(1)} + \frac{(\sigma + \alpha_2)(\mu + \alpha_2) - \mu\sigma}{D_2}k_1 = 0.$$

This is a linear equation with constant coefficients; therefore the solution is readily determined and is exponentially bounded. The coefficients are determined by the usual conditions, i.e., the kernel has to integrate to unity, it has to be continuous at zero, and the jump conditions at zero have to be satisfied.

Appendix C. Proof of Theorem 3.1. The exponential ansatz $u(t, x) = \exp(\lambda t)\phi(x)$ in the linearization (3.6) leads to the eigenvalue problem

(C.1)
$$\nu\phi(x) = I[\phi](x) = \int_0^L k(x, y)\phi(y)dy$$

with $\nu = \lambda + 1 - r$. The solution u of (3.6) will grow if $\lambda > 0$ and decay if $\lambda < 0$. Hence, the critical value is given by $\lambda = 0$ or $\nu = 1 - r$.

We now show that the dominant eigenvalue ν^* is a monotone increasing function of domain length. For two domain lengths $L_2 > L_1$, we denote I_j as the linear operator given by (C.1) with L replaced by L_j, $j = 1, 2$. We denote $\nu_{1,2}$ as the corresponding dominant eigenvalues and $\phi_{1,2}$ as corresponding (positive) eigenfunctions. Then $I_2 \geq I_1$ and hence $\nu_2 \geq \nu_1$. We show that the inequality is in fact strict. We write

$$I_2\phi_2 = I_1\phi_2 + \int_{L_1}^{L_2} k(x,y)\phi_2(y)dy.$$

Since $\phi_2 > 0$, the last term is positive and hence there is an $\varepsilon > 0$ such that

$$f := \int_{L_1}^{L_2} k(x,y)\phi_2(y)dy > \varepsilon\phi_1.$$

Then the equation $\nu_2\psi = I_1\psi + f$ has no solution for $\nu_2 \leq \nu_1$ [21]. But ϕ_2 is a solution and hence necessarily $\nu_2 > \nu_1$.

If the dispersal kernel is continuous, then the resulting integral operator on $\mathcal{L}^2[0,L]$ is completely continuous and, for positive kernel, has a unique simple dominant eigenvalue [21]. Therefore, our assumptions are valid for all kernels in sections 4 and 5. In fact, the condition that the kernel be continuous can be weakened by saying that the kernel to the power $1 + q$, $q \geq 1$, has to be integrable on $[0,L]^2$ [21]. Numerically, the fat-tailed kernel (2.7) can be bounded by $x^{-0.4}$, which is square integrable, and hence the assumption holds. This is an area of future research.

Appendix D. Proof of Theorem 3.2. By scaling time, we may assume $\mu = 1$ in (3.1). It was shown in [26] that $c^- \leq c^*_-$ and $c^*_+ \leq c^+$. To show the reversed inequalities, we follow Aronson's proof [2] and show that for all $c \in (c^-, c^+)$ there is a subsolution of (3.1) which expands at speed c. Due to a comparison principle, the true solution has to expand at speed at least c.

We make the following technical requirements on the kernel k [2]. We assume $k \geq 0$ and $\text{supp}(k) = \mathbb{R}$. We assume that the moment generating function $M(s)$ exists for $s \in (\hat{s}^-, \hat{s}^+)$ with $\hat{s}^- < 0$, $\hat{s}^+ > 0$. We assume furthermore that the function

$$\text{(D.1)} \qquad A_\lambda(s) = [(M(s) + \lambda)/s], \qquad s \neq 0,$$

has exactly one minimum at $\bar{s}^+ \in (0, \hat{s}^+)$ and one maximum at $\bar{s}^- \in (\hat{s}^-, 0)$. In addition, $A_\lambda(s)$ is increasing on $(\hat{s}^-, \bar{s}^-) \cup (\bar{s}^+, \hat{s}^+)$ and decreasing on $(\bar{s}^-, 0) \cup (0, \bar{s}^+)$. Finally, we assume that the function $x \mapsto \exp(sx)k(x)$ is decreasing for large enough x. Note that with this notation, $c^\pm = A_\lambda(\bar{s}^\pm)$ with $\lambda = f'(0) - 1$.

We first switch to a moving coordinate frame and show a comparison principle for the resulting integrodifferential operator. The function $W(t,\xi) = u(t, \xi + ct)$ satisfies

$$\text{(D.2)} \quad W_t = cW_\xi + f(W) - W + \int k(\xi - \eta)W(t, \eta)d\eta =: Q_c[W], \quad W(0, \xi) = u(0, \xi).$$

LEMMA D.1 (comparison). *Let V, W be bounded and continuously differentiable functions which satisfy, on $\mathbb{R}^+ \times \mathbb{R}$,*

$$\text{(D.3)} \qquad V_t - Q_c[V] \geq W_t - Q_c[W],$$

and $V(0, \xi) > W(0, \xi)$ on $\mathbb{R}$. Then $V > W$ on $(0, \infty) \times \mathbb{R}$.

Proof. Let V, W be given. The difference $Z = V - W$ satisfies

$$\text{(D.4)} \qquad Z_t - cZ_\xi \geq h(t, \xi)Z + k * Z, \quad Z(0, \cdot) > 0,$$

where h is some bounded function, given by the mean value theorem. Suppose there is a first time t_0 such that $Z > 0$ on $[0, t_0) \times \mathbb{R}$, and $Z(t_0, \xi_0) = 0$ for some ξ_0. By assumption, the convolution term in (D.4) is nonnegative on $[0, t_0] \times \mathbb{R}$. Therefore, along the characteristic lines $\xi + ct$, Z is bounded below by the solution of the differential equation $\dot{\zeta} = h\zeta$, $\zeta(0, \xi) = Z(0, \xi) > 0$. Since ζ remains positive, Z has to remain positive. $\quad\square$

In the following, we will use Lemma D.1 with nonstrict inequalities, i.e., $V(0, \xi) \geq W(0, \xi)$ implies $V \geq W$, provided V satisfies a well-posed initial value problem, and still refer to that as Lemma D.1. The idea is the same as in [2]. Let V_ϵ, $\epsilon > 0$, be the solution of a well-posed initial value problem with initial value $V_\epsilon(0, \xi) = V(0, \xi) + \epsilon$. Then by the above $V_\epsilon > W$, and in the limit $\epsilon \to 0$, we have $V \geq W$.

LEMMA D.2 (subsolution). *Let $c \in (c^-, c^+)$ be given. Then there exists a function $V_0(\xi)$, which is positive on $(0, \pi/\gamma)$, such that $Q_c[\varepsilon V_0] \geq 0$ and*

$$\text{(D.5)} \qquad Q_c[\varepsilon V_0] > 0 \quad on \quad (0, \pi/\gamma)$$

for all sufficiently small $\varepsilon, \gamma > 0$.

Before we prove Lemma D.2, we demonstrate how the subsolution and repeated use of the comparison principle are employed to prove the theorem. Suppose that $W(0, \xi)$ and $c \in (c^-, c^+)$ are given and $W(t, \xi)$ satisfies (D.2). We need to show that $W(t, \xi) \to \bar{u}$ as $t \to \infty$ for all $\xi \in \mathbb{R}$. At first, Lemma D.2 ensures the existence of $V_0(\xi)$, which is positive on $(0, \pi/\gamma)$ for small enough $\gamma > 0$. We apply the comparison principle to εV_0 and V, defined as the solution to

$$\text{(D.6)} \qquad V_t = Q_c[V], \qquad V(0, \xi) = \varepsilon V_0(\xi),$$

to see that $V(t, \xi) \geq \varepsilon V_0(\xi)$ for all $t > 0$. Next, the comparison principle is applied to $V(t, \xi)$ and $\tilde{V}(t, \xi) = V(t + h, \xi)$ for any fixed $h > 0$. As a result, $\tilde{V} \geq V$ and therefore $V(t, \xi)$ is a nondecreasing function in t for each fixed ξ. On comparing $V(t, \xi)$ with the constant $\bar{u}$, we get that V is bounded by $\bar{u}$, and therefore $V(t, \xi) \to q(\xi)$ for each ξ. Following Aronson [2], one can actually show that $q(\xi) \equiv \bar{u}$.

Finally, for T sufficiently large, there is a bound $m > 0$ such that $W(T, \xi) \geq m > 0$ on $(0, \pi/\gamma)$. We choose $\varepsilon > 0$ such that $\varepsilon V_0 < m$. We now apply the comparison principle to $W(t, \xi)$ and the solution $V(t - T, \xi)$ of $V_t = Q_c[V]$, $V(T, \xi) = \varepsilon V_0(\xi)$, to obtain that $W(t, \xi) \geq V(t - T, \xi)$. This completes the proof.

We now prove Lemma D.2. We first look at the linear equation

$$\text{(D.7)} \qquad W_t = L_c[W] := cW_\xi + \lambda W + k * W,$$

where $*$ denotes the convolution. For $s \in (\bar{s}^-, \bar{s}^+) \backslash \{0\}$, we define

$$\text{(D.8)} \qquad \hat{V}_0(\xi) = e^{-s\xi} \sin \gamma \xi.$$

After a little bit of algebra, we find that $L_c[\hat{V}_0](\xi)$ is given by

$$\left[-cs + \lambda + \int e^{s\eta} k(\eta) \cos(\gamma\eta) d\eta \right] \hat{V}_0 + \left[c\gamma - \int e^{s\eta} k(\eta) \sin(\gamma\eta) d\eta \right] e^{-s\xi} \cos \gamma \xi.$$

Therefore, $L_c[\hat{V}_0] > 0$ on $(0, \pi/\gamma)$ if the following three conditions are satisfied:

$$(D.9) \qquad c < \frac{1}{s}\left[\lambda + \int e^{s\eta}k(\eta)\cos(\gamma\eta)d\eta\right] =: \mathcal{A}_\lambda(s, \gamma), \qquad s > 0,$$

$$(D.10) \qquad c > \mathcal{A}_\lambda(s, \gamma), \qquad s < 0,$$

$$(D.11) \qquad c = \frac{1}{\gamma}\left[\int e^{s\eta}k(\eta)\sin(\gamma\eta)d\eta\right] =: \mathcal{B}(s, \gamma).$$

We first establish some properties of the functions $\mathcal{A}_\lambda$ and $\mathcal{B}$. As $\gamma \to 0$, we have uniform convergence on compact subsets of $(\bar{s}^-, \bar{s}^+)\backslash\{0\}$ of

$$\mathcal{A}_\lambda(s, \gamma) \to A_\lambda(s), \quad \mathcal{B}(s, \gamma) \to B(s): = \int \eta e^{s\eta}k(\eta)d\eta.$$

The function $B(s)$ is increasing. Differentiation gives $A'_\lambda(s) = (B(s) - A_\lambda(s))/s$. Hence, due to the assumptions on A_λ, we furthermore see that $B < A_\lambda$ on $(0, \bar{s}^+)$, $B > A_\lambda$ on $(\bar{s}^-, 0)$, and $B(\bar{s}^\pm) = A_\lambda(\bar{s}^\pm)$. Note that $B(0)$ is the average dispersal distance, and since B is an increasing function, $c^- < B(0) < c^+$; i.e., the interval (c^-, c^+) is never empty.

We now return to the construction of $\hat{V}_0$; i.e., we show that conditions (D.9)–(D.11) can be satisfied simultaneously. Without loss of generality, we may assume $c > B(0)$, and hence we restrict ourselves to $s > 0$. First, we can choose $\lambda < f'(0) - 1$ such that $c < A_\lambda(\bar{s}^+)$. Then we can choose $s_0, s_1, \delta, \gamma > 0$, such that

$$B(s_0) + \delta < c < B(s_1) - \delta \quad \text{and} \quad |\mathcal{B}(s, \gamma) - B(s)| < \delta.$$

By continuity, there is a value $s(\gamma)$ such that $\mathcal{B}(s(\gamma), \gamma) = c$ for all sufficiently small γ. Obviously, we can choose γ small enough such that $\mathcal{A}_\lambda(s(\gamma), \gamma) > c$. Hence, the two conditions (D.9), (D.11) can be satisfied simultaneously.

By the same argument as [2], one can show that the modified function

$$(D.12) \qquad V_0(\xi) = \hat{V}_0(\xi), \quad \xi \in [0, \pi/\gamma], \quad V_0(\xi) = 0, \quad \xi > \pi/\gamma,$$

also satisfies $L_c[V_0] > 0$ on $(0, \pi/\gamma)$.

As a last step, we have to show that for small enough $\varepsilon > 0$ we have $Q_c[\varepsilon V_0] > 0$ on that same interval. Note that $\lambda < f'(0) - 1$ implies that $\lambda\varepsilon < f(\varepsilon) - \varepsilon$ for small enough $\varepsilon > 0$. Hence, we have $Q_c[\varepsilon V_0] > L_c[\varepsilon V_0] > 0$ on $(0, \pi/\gamma)$, which completes the proof.

Appendix E. The Advection Diffusion Kernel for Bounded Domains. Movement is modeled by (4.1) on the interval $[-L/2, L/2]$ with initial condition $z(0, x) = \delta(x - y)$. The boundary conditions are

$$(E.1) \qquad \left(z_x - \frac{v}{D}z\right)(t, -L/2) = 0, \qquad z(t, L/2) = 0.$$

We interpret these conditions as a stream where individuals cannot enter or leave at the upstream end and are washed out at the downstream end [37]. We nondimensionalize (4.1) by setting $X = x/L$, $T = \alpha t$, $Z = Lz$, which gives

$$(E.2) \qquad Z_T = \frac{1}{\tilde{L}^2}Z_{XX} - \tilde{v}Z - Z, \quad Z(T, 1/2) = 0 = (Z_X - \tilde{L}^2\tilde{v}Z)(T, -1/2),$$

where $\tilde{L}^2 = \alpha L/D$ and $\tilde{v} = v/(\alpha L)$. For convenience, we write the variables t, x in lowercase letters again. We want to find the nondimensional kernel given by $\kappa(x, y) = \int_0^\infty \alpha Z(t, x) dt$. The function $W(t, x) = \exp(-L^2 vx/2) Z(t, x)$ satisfies

$$\text{(E.3)} \qquad W_t = \frac{1}{L^2} W_{xx} - \beta W,$$

where $\beta = 1 + \frac{v^2 L^2}{4}$. Separating variables $W(t, x) = T(t)X(x)$, we get the two independent equations $T' = -(\lambda^2 + \beta)T$ and $X'' = -\lambda^2 L^2 X$ for some $\lambda^2 > 0$. The boundary conditions applied to the equations for X result in the defining condition

$$\text{(E.4)} \qquad \lambda = -\frac{vL}{2} \tan(\lambda L).$$

We denote its infinitely many (symmetric) nonzero solutions by λ_n, $n = 1, 2, \ldots$. The corresponding family of orthogonal solutions is given by

$$\text{(E.5)} \qquad \phi_n(x) = -\tan(\lambda_n L/2) \cos(\lambda_n Lx) + \sin(\lambda_n Lx)$$

with norm

$$\|\phi_n\|_2^2 = \frac{1}{2}(1 + \tan^2(\lambda_n L/2)).$$

The solution of (E.3) can hence be written as an infinite sum where each term is of the form $c_n e^{-(\lambda_n + \beta)t} \phi_n(x)$. To find expressions for the coefficients c_n we approximate the delta distribution by the top hat function,

$$\delta_m(x - y) = \begin{cases} 2m, & |x - y| \leq 1/m, \\ 0, & \text{else.} \end{cases}$$

Expanding the approximate initial condition

$$\delta_m(x - y) e^{-\frac{vL^2}{2}x} = \sum c_n \phi_n(x)$$

and using the intermediate value theorem gives

$$c_n = \frac{e^{-\frac{vL^2}{2}y} \phi_n(y)}{\|\phi_n\|_2^2}.$$

Hence, the nondimensionalized kernel is given by

$$\text{(E.6)} \qquad k(x, y) = e^{-\frac{vL^2}{2}(y-x)} \sum_n \frac{1}{\lambda_n^2 + 1 + \frac{v^2 L^2}{4}} \frac{2}{1 + \tan^2(\frac{\lambda_n L}{2})} S(x)S(y),$$

where $S(x) = (\sin(\lambda_n Lx) - \tan(\lambda_n L/2) \cos(\lambda_n Lx))$. In Figure E.1 we plot this kernel for three different advection speeds.
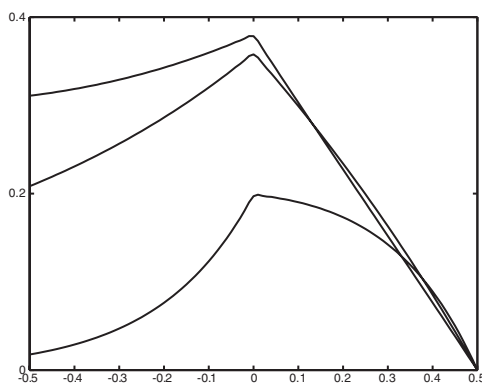
Fig. E.1 *The kernel with advection, no-flux boundary conditions at the left end, zero boundary conditions at the right end, release point in the middle, for $v = 0.2$ (top curve), $v = 1$ (middle), and $v = 5$ (bottom).*

Appendix F. Exact Derivation of the Critical Domain Length. We determine the critical domain length for the kernel (4.4) by computing the eigenvalue of the corresponding integral operator (C.1), extending earlier work [20, 41]. Scaling the space variable by L gives

$$\text{(F.1)} \qquad \nu\phi(x) = \int_0^1 \tilde{\kappa}(x,y)\phi(y)dy,$$

where $\tilde{\kappa}$ is defined as κ with a_j, A replaced by $b_j = La_j$, $B = LA$. Differentiating (F.1) gives

$$\text{(F.2)} \qquad \nu\phi'(x) = b_2\nu\phi(x) + (b_1 - b_2)\int_x^1 Be^{b_1(x-y)}\phi(y)dy.$$

Differentiating again, we obtain

$$\text{(F.3)} \qquad \nu\phi''(x) = (b_2 - b_1)B\phi(x) + b_2^2\nu\phi(x) + (b_1^2 - b_2^2)\int_x^1 Be^{b_1(x-y)}\phi(y)dy.$$

Substituting (F.2) into (F.3), we get the regular Sturm–Liouville problem
(F.4)
$$\phi''(x) = -b_1|b_2|\left(\frac{1}{\nu} - 1\right)\phi(x) + (b_1 + b_2)\phi'(x), \quad \phi'(0) = b_1\phi(0), \quad \phi'(1) = b_2\phi(1).$$

We apply the transformation $\psi(x) = \exp(-\frac{b_1+b_2}{2}x)\phi(x)$ to (F.4) and substitute the original parameters back to obtain

$$\text{(F.5)} \qquad \psi'' = -L^2\frac{(a_1 - a_2)^2}{4}\left(\frac{4a_1|a_2|}{\nu(a_1 - a_2)^2} - 1\right)\psi,$$

together with the boundary conditions

$$\text{(F.6)} \qquad \psi'(0) = L\frac{a_1 - a_2}{2}\psi(0) \qquad \text{and} \qquad \psi'(1) = -L\frac{a_1 - a_2}{2}\psi(1).$$

Equations (F.5) and (F.6) constitute a Sturm–Liouville problem, which one can solve for L as a function of ν [41], and the solution is given by formula (4.6).

Acknowledgment. The authors thank Roger Nisbet for insightful discussions and helpful comments.

REFERENCES

[1] J. ALLAN, *Stream Ecology: Structure and Function of Running Waters*, Chapman & Hall, London, 1995.

[2] D. ARONSON, *The asymptotic speed of propagation of a simple epidemic*, in Nonlinear Diffusion, W. Fitzgibbon and H. Walker, eds., Res. Notes Math. 14, Pitman, London, 1977, pp. 1–23.

[3] D. ARONSON AND H. WEINBERGER, *Nonlinear diffusion in population genetics, combustion, and nerve pulse propagation*, in Partial Differential Equations and Related Topics, J. Goldstein, ed., Lecture Notes in Math. 446, Springer-Verlag, Berlin, 1975, pp. 5–49.

[4] R. BAKER AND P. DUNN, *New Directions in Biological Control*, Alan Liss, New York, 1990.

[5] M. BALLYK AND H. SMITH, *A model of microbial growth in a plug flow reactor with wall attachment*, Math. Biosci., 158 (1999), pp. 95–126.

[6] L. W. BOTSFORD, A. HASTINGS, AND S. D. GAINES, *Dependence of sustainability on the configuration of marine reserves and larval dispersal distance*, Ecology Lett., 4 (2001), pp. 144–150.

[7] S. R. BROADBENT AND D. G. KENDALL, *The random walk of* Trichostrongylus retortaeformis, Biometrica, 9 (1953), pp. 460–466.

[8] R. S. CANTRELL AND C. COSNER, *Should a park be an island?*, SIAM J. Appl. Math., 53 (1993), pp. 219–252.

[9] R. S. CANTRELL AND C. COSNER, *On the effects of spatial heterogeneity on the persistence of interacting species*, J. Math. Biol., 37 (1998), pp. 103–145.

[10] D. CARRERO, G. MCDONALD, E. CRAWFORD, G. DE VRIES, AND M. HENDZEL, *Using FRAP and mathematical modeling to determine the in vivo kinetics of nuclear proteins*, Methods, 29 (2003), pp. 14–28.

[11] R. GORENFLO AND F. MAINARDI, *Approximation of Lévy-Feller diffusion by random walk*, Z. Anal. Anwendungen, 18 (1999), pp. 231–246.

[12] K. HADELER, *Reaction transport systems*, in Mathematics Inspired by Biology, CIME Lectures 1997, Florence, V. Capasso and O. Diekmann, eds., Springer-Verlag, New York, 1998, pp. 95–150.

[13] K. HADELER AND M. LEWIS, *Spatial dynamics of the diffusive logistic equation with sedentary component*, Canad. Appl. Math. Quart., 10 (2004), pp. 473–500.

[14] T. HILLEN, *Transport equations with resting phase*, European J. Appl. Math., 14 (2003), pp. 613–636.

[15] E. HOLMES, M. LEWIS, J. BANKS, AND R. VEIT, *Partial differential equations in ecology: Spatial interactions and population dynamics*, Ecology, 75 (1994), pp. 117–129.

[16] V. HUTSON, S. MARTINEZ, K. KISCHAIKOW, AND G. VICKERS, *The evolution of dispersal*, J. Math. Biol., 46 (2003), pp. 483–517.

[17] H. KIERSTEAD AND L. B. SLOBODKIN, *The size of water masses containing plankton blooms*, J. Marine Res., 12 (1953), pp. 141–147.

[18] A. KOLMOGOROV, I. PETROVSKII, AND N. PISKUNOV, *A study of the equation of diffusion with increase in the quantity of matter, and its application to a biological problem*, Bjol. Moskovskovo Gos. Univ., 17 (1937), pp. 1–72.

[19] M. KOT, M. LEWIS, AND P. VAN DEN DRIESSCHE, *Dispersal data and the spread of invading organisms*, Ecology, 77 (1996), pp. 2027–2042.

[20] M. KOT AND W. M. SCHAFFER, *Discrete-time growth-dispersal models*, Math. Biosci., 80 (1986), pp. 109–136.

[21] M. A. KRASNOSEL'SKII, *Positive Solutions of Operator Equations*, Noordhoff, Groningen, The Netherlands, 1964.

[22] J. LANCASTER AND A. HILDREW, *Characterising instream flow refugia*, Canad. J. Fish. Aquat. Sci., 50 (1993), pp. 1663–1675.

[23] M. LEWIS AND G. SCHMITZ, *Biological invasion of an organism with separate mobile and stationary states: Modeling and analysis*, Forma, 11 (1996), pp. 1–25.

[24] D. LOCKWOOD, A. HASTINGS, AND L. BOTSFORD, *The effects of dispersal patterns on marine reserve: Does the tail wag the dog?*, Theor. Popul. Biol., 61 (2002), pp. 297–309.

[25] F. LUTSCHER AND M. A. LEWIS, *Spatially-explicit matrix models. A mathematical analysis of stage-structured integrodifference equations*, J. Math. Biol., 48 (2004), pp. 293–324.

[26] J. MEDLOCK AND M. KOT, *Spreading diseases: Integro-differential equations new and old*, Math. Biosci., 184 (2003), pp. 201–222.

[27] K. MÜLLER, *Investigations on the Organic Drift in North Swedish Streams*, Tech. report 34, Institute of Freshwater Research, Drottningholm, Sweden, 1954.

[28] K. MÜLLER, *The colonization cycle of freshwater insects*, Oecologica, 53 (1982), pp. 202–207.

[29] J. MURRAY AND R. SPERB, *Minimum domains for spatial patterns in a class of reaction diffusion equations*, J. Math. Biol., 18 (1983), pp. 169–184.

[30] M. G. NEUBERT, M. KOT, AND M. A. LEWIS, *Dispersal and pattern formation in a discrete-time predator-prey model*, Theoret. Population Biol., 48 (1995), pp. 7–43.

[31] H. OTHMER, S. DUNBAR, AND W. ALT, *Models of dispersal in biological systems*, J. Math. Biol., 26 (1988), pp. 263–298.

[32] A. OKUBO AND S. A. LEVIN, *Diffusion and Ecological Problems: Modern Perspectives*, Springer-Verlag, New York, 2001.

[33] E. PACHEPSKY, F. LUTSCHER, R. NISBET, AND M. A. LEWIS, *Persistence, spread and the drift paradox*, Theoret. Population Biol., 67 (2005), pp. 61–73.

[34] G. SKALSKI AND J. GILLIAM, *A diffusion-based theory of organism dispersal in heterogeneous populations*, Amer. Nat., 161 (2003), pp. 441–458.

[35] J. G. SKELLAM, *Random dispersal in theoretical populations*, Biometrika, 38 (1951), pp. 196–218.

[36] H. SMITH AND P. WALTMAN, *The Theory of the Chemostat*, Cambridge University Press, Cambridge, UK, 1995.

[37] D. SPEIRS AND W. GURNEY, *Population persistence in rivers and estuaries*, Ecology, 82 (2001), pp. 1219–1237.

[38] R. SYSKI, *Random Processes*, Marcel Dekker, New York, 1989.

[39] H. THIEME AND X.-Q. ZHAO, *Asymptotic spreads of speed and traveling waves for integral equations and delayed reaction-diffusion models*, J. Differential Equations, 195 (2003), pp. 430–470.

[40] P. TURCHIN, *Quantitative Analysis of Movement*, Sinauer, Sunderland, MS, 1998.

[41] R. W. VAN KIRK AND M. A. LEWIS, *Integrodifference models for persistence in fragmented habitats*, Bull. Math. Biol., 59 (1997), pp. 107–137.

[42] R. WATERS, *The drift of stream insects*, Ann. Rev. Entomol., 17 (1972), pp. 253–272.